International Symposium
On Turbulence and Shear Flow
Phenomena (TSFP-9)
June 30 - July 3, 2015 *Melbourne, Australia*

USE OF PROPER ORTHOGONAL DECOMPOSITION TO INVESTIGATE THE TURBULENT WAKE OF A SURFACE-MOUNTED FINITE SQUARE PRISM

Rajat Chakravarty, Nader Moazamigoodarzi, Donald J. Bergstrom and David Sumner
Department of Mechanical Engineering
University of Saskatchewan
57 Campus Drive, Saskatoon, Saskatchewan, S7N 5A2, Canada
rajat.c@usask.ca

ABSTRACT

This study aims to investigate the characteristics of the instantaneous velocity field in select vertical planes located in the turbulent wake of a surface-mounted finite square prism. The instantaneous velocity field is obtained from a Large Eddy Simulation (LES); state-of-the-art post-processing methodologies namely the Proper Orthogonal Decomposition (POD) and the swirling strength criterion are used to analyse the flow structure. The study specifically considers the flow over a square prism of aspect ratio AR = 3 (AR = H/D where H is the height and D is the prism width) mounted on a ground plane and located within a thin laminar boundary layer. The Reynolds number based on the freestream velocity and cylinder width is Re = 500, and the angle of incidence is zero. POD is used to extract the dominant flow features, especially those related to vortex shedding, while the swirling strength criterion is used to visualise the small-scale turbulent structures. A principal conclusion of the study is that strong periodicity is observed in a transverse plane located 3.5D downstream of the prism, whereas the vertical mid-plane revealed a more complicated periodic structure. No compelling evidence of half-loop structures was obtained based on the analysis of the flow for a single periodic cycle. On the other hand, strong streamwise vortex structures were observed in the transverse plane in the upper region of the wake, somewhat reminiscent of but not the same as tip vortices.

INTRODUCTION

Flows over surface-mounted square prisms have been extensively studied in the literature. This flow is not only relevant from an industrial perspective in terms of flow over buildings and chimneys, but also from a research standpoint as the flow around the prism/cylinder and its turbulent wake exhibit multiple complex features. Many studies in the literature have focused on the time-averaged features of this flow, with relatively fewer studies investigating the instantaneous topologies of the flow field.

While heuristic approaches have identified the different regions of the prism wake, some recent studies have attempted to propose a unifying flow theory based on the dynamics of the vortical structures shed from the prism. Wang and Zhou [1] suggested that the instantaneous flow tends to form arch-type vortices regardless of aspect ratio and is characterized by two spanwise vertical 'legs' perpendicular to the ground plane and a connecting horizontal 'bridge' at the free end. Based on probabilistic analysis and two-dimensional (2D) Particle Image Velocimetry (PIV) measurements, they developed a model of an outward-bulging arch vortex, which explains some of the mean flow characteristics in the wake downstream of the finite prism. More recently, Bourgeois et al. [2] proposed a different flow paradigm, namely the alternating half-loop vortex structure shed by the finite square prism into the wake. They indicated that the mean flow structure of the wake could be explained by averaging the quasi-periodic half-loop structure over the shedding period. A schematic of the alternating half-loop vortex structure is given in Figure 1. A single half-loop structure is made up of a principal core which is aligned approximately perpendicular to the ground plane and a streamwise connector strand. The strand connects the top of the principal core to the base of the principal core of the next half-loop located upstream. Since the principal cores occur on alternate sides of the wake, each connector strand stretches diagonally across the wake, with an orientation which also alternates. A detailed description of the half-loop and educed phase-averaged structure can be found in [2].

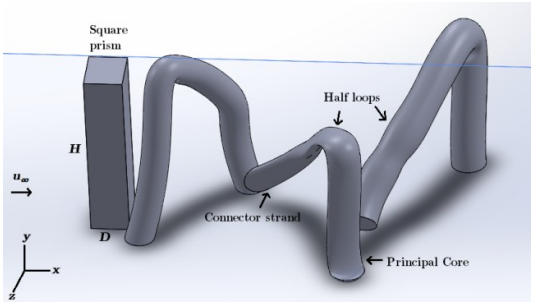

Figure 1. Schematic for the alternating half-loop structures in the wake of a surface-mounted square prism.

Both of the studies above considered finite square prisms of larger aspect ratio for relatively higher Reynolds numbers. Saha [3] studied the flow past a finite-height surface-mounted square prism using direct numerical simulation (DNS) at a lower Reynolds number of Re = 250 for four different aspect ratios: AR = 2, 3, 4 and 5.

Without trying to propose a unifying theory, Saha [3] observed tip vortices, base vortices and horseshoe vortices in the prism wake regardless of aspect ratio. For AR > 2, the near-wake shows a symmetric shear layer separation while the far-wake shows greater anti-symmetric vortex shedding characteristics.

All the above studies consider different Reynolds numbers and inflow boundary conditions, which can have a dramatic effect on the characteristics of their respective wakes. From the above literature, it is also clear that a better understanding of the instantaneous turbulent structures in the wake of this flow field would be helpful. In the present investigation, we consider a relatively short prism, i.e. AR = 3, and a low Reynolds number, i.e. Re = 500. The prism is immersed in a thin laminar boundary layer. The resolved-scale velocity and pressure fields are obtained from a large eddy simulation (LES) of the flow. Subsequent analysis focuses on the instantaneous velocity field in two vertical planes within the prism wake: the vertical mid-plane, and one transverse plane located 3.5D downstream of the square prism. Both the POD and visualisation based on the swirling strength criterion will be used to draw insight into the vortical structures shed by the prism into the wake and explore its periodic behaviour. If the half-loop structure exists in the present flow, then the velocity fields in both planes should show evidence of the half-loop, and especially the connector strand, as it is convected downstream in the wake.

NUMERICAL SCHEME AND POST-PROCESSING METHODS

A finite volume discretization of the filtered Navier-Stokes equations was used as the computational model for this flow. The momentum equations were discretized in time using the Crank-Nicholson method, and the subsequent set of linear equations was solved using the fractional step method. An algebraic multigrid method was used to accelerate the solution of the pressure-correction equation. The subgrid-scale (SGS) stress terms were modeled using a localised Dynamic Smagorinsky model. A structured, Cartesian grid with 128 x 144 x 96 control volumes in the x (freestream), y (spanwise) and z (transverse) direction, respectively, was used to discretize the flow domain. The prism was located approximately 3D from the inlet plane and the blockage ratio was about 7%. The approaching boundary layer on the ground plane was laminar and relatively thin.

A snap-shot POD analysis [4] of the instantaneous velocity fields in the transverse plane at z/D = 0, and one freestream plane at x/D = 3.5 was performed. The POD methodology can be used to extract motions of different scales within the evolving dynamics of a flow. The POD is applied to decompose the time-dependent fluctuating part of the flow field into an orthonormal system of spatial modes or eigenfunctions, $v_m(x)$, and associated temporal coefficients $a_m(t)$, i.e.

$$v(x_i,t) = v_o(x_i) + \sum_{m=1}^{M} a_m(t) v_m(x_i) \qquad (1)$$

The coefficients are obtained from the solution of an eigenvalue problem based on the covariance matrix of the velocity field. The relative magnitude of the eigenvalues (λ_m) determines the respective energy contributions in each mode. Finally, the POD modes are computed as

$$v_m(x_i) = \frac{1}{M\lambda_m} \sum_{n=1}^{M} a_m(t_n)\, v(x_i,t_n) \qquad (2)$$

In this case, 100 snapshots of the time-resolved fluctuating velocity field equally distributed in time across approximately one shedding cycle of the flow were used to provide the data base for POD analysis. The temporal coefficients obtained from the POD analysis were also analysed to investigate the periodic features of this flow. Following van Oudheusden et al. [5], the POD temporal coefficients of the first two energy modes allow for a direct phase identification of the flow field. The phase angle φ_i is obtained when the first two normalized POD coefficients are plotted on a plane. This allows for a phase-sorted representation of one shedding period of the wake i.e.

$$\frac{a_1(i)}{\sqrt{2\lambda_1}} = r_i \sin(\varphi_i) \quad \frac{a_2(i)}{\sqrt{2\lambda_2}} = r_i \cos(\varphi_i) \qquad (3)$$

where the normalized ellipse has a radius given by

$$r_i^2 = \left(\frac{a_1(i)}{\sqrt{2\lambda_1}}\right)^2 + \left(\frac{a_2(i)}{\sqrt{2\lambda_2}}\right)^2 \qquad (4)$$

Chong et al. [6] defined vortices as regions where the local velocity gradient tensor has complex-conjugate eigenvalues. In this study, 2D velocity field data were used to obtain localized velocity gradients. Regions where complex-conjugate eigenvalues were found, were concluded to contain localized vortex structures.

SELECTED RESULTS AND DISCUSSION

Only a few studies in the literature have investigated such flows from the standpoint of studying the instantaneous flow features and the turbulence structures associated with this rather simple flow configuration. The selected results shown in this section will investigate the effect of the coherent structures in the wake on the instantaneous flow field in a transverse plane, and to a lesser extent the mid-plane, based on the data extracted over approximately one periodic cycle.

Time-averaged Flow Patterns

Before studying the instantaneous wake characteristics of this flow field, it is helpful to review the time-averaged or mean flow structure, in particular how it differs from similar flow fields at different aspect ratios and Reynolds numbers. Figure 2 shows the mean streamlines with transverse vorticity contours superimposed in the vertical

mid-plane of the wake of the square prism. The flow is characterized by a separation from the leading edge of the free end of the prism. The shear layer formed does not reattach to the free end, but instead connects to a large recirculation zone located in the upper half of the near-wake. For the mean flow field, a dividing streamline represents the boundary between the fluid recirculating in the near-wake and the fluid being convected into the downstream region of the wake. At the junction of the prism with the ground plane we also see two smaller vortices on the front and rear faces of the prism. The vortex on the upstream face relates to the horseshoe vortex, which wraps around the base of the prism and is located on the ground plane.

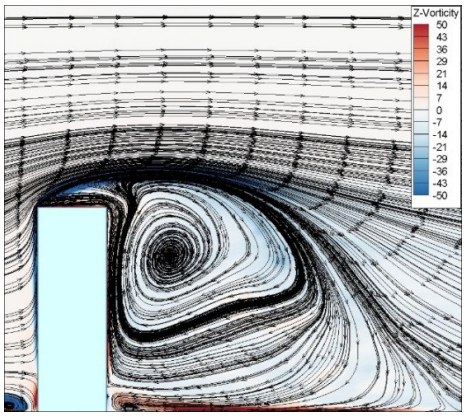

Figure 2. Mean streamlines with contours of transverse vorticity superimposed for the vertical mid-plane of the wake.

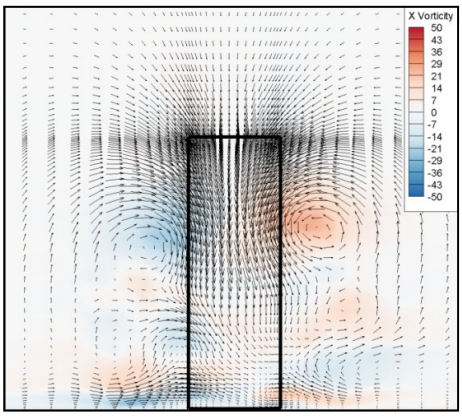

Figure 3. Mean velocity vectors and contours of streamwise vorticity for a transverse vertical section located at $x/D = 3.5$.

Figure 3 shows the mean velocity vectors overlaid with contours of streamwise vorticity in a transverse plane located downstream of the square prism at $x/D = 3.5$. Two strong counter-rotating vortices are observed on either sides of the prism. Their location near the top of the prism has them sometimes referred to as tip vortices. These vortices create a strong downwash velocity component along the vertical centerline. Additionally we notice some weaker streamwise vortices in the lower region of the wake. Note that the lack of symmetry may indicate that the time interval used for averaging is too small. The lack of strong base vortex structures and the associated upwash flow may be due to the thin laminar boundary layer on the ground plane. Relatively weak vortex structures are also observed at the junction with the ground plane.

POD and Swirling Strength Criterion Results

As would be expected, POD was able to capture the dominant mechanisms of the fluctuating velocity fields with only a few energy modes as shown in Figure 4. Across both planes, the first energy mode captured 18-28% of the total energy, with the first 10 modes cumulatively capturing close to 90% of the total energy. In both planes, the cumulative energy captured by the first two energy modes is around 35-50%. For the transverse plane, the energy distribution is consistent with the findings of Wang et al. [8], which suggested a coupling in the first two pairs of energy modes due to the presence of asymmetric and symmetric vortex shedding tendencies in these modes, respectively. Note that whereas for the transverse plane, there is a very distinct drop in energy within the first four modes, for the mid-plane the energy content of the first four modes is much more uniform.

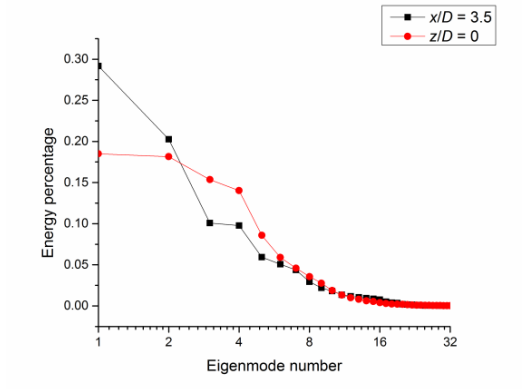

Figure 4. POD energy distribution percentage for the $z/D = 0$ and $x/D = 3.5$ planes

Recall that POD provides for an orthonormal decomposition of a set of instantaneous velocity fields into a basis of eigenmodes (or energy modes) of decreasing energy content. Figure 5 shows the first and second POD energy modes for the flow in the transverse plane at $x/D = 3.5$. For both modes, strong vortex structures occur in the wake of the prism, resulting in flows which tend to sweep laterally across the prism. For the first mode, Figure 5(a), the predominant direction is from left to right, whereas for the second mode, Figure 5(b), the direction is reversed, except for a strong outflow on the right hand side near the ground plane. Typically, larger vortex structures occur near the top and along the lateral edges, with smaller structures near the ground plane.

The variation of the POD temporal coefficients indicated strong periodicity of the flow in the x/D = 3.5 plane, which was not expected for such a low aspect ratio prism. This strong periodicity was not evident when the corresponding coefficients for the transverse mid-plane were analyzed. Analysis of the first four temporal coefficients yields a dominant frequency that corresponds to a Strouhal number of St = 0.127, which is in close agreement with the value found by previous studies [9]. Figure 6 shows a plot of the first two normalized temporal coefficients $a_1^* = a_1/(r_i(2\lambda_1))^{1/2}$ v/s $a_2^* = a_2/(r_i(2\lambda_2))^{1/2}$ for the x/D = 3.5 plane. These points are distributed on the unit circle; each point on the circle corresponds to the phase angle of the vortex shedding motion. A similar plot for the mid-plane (not shown) did not reveal similar periodic behaviour.

POD is also helpful in isolating the most energetic structures in a flow field by using a lower-order reconstruction of the most energetic modes.

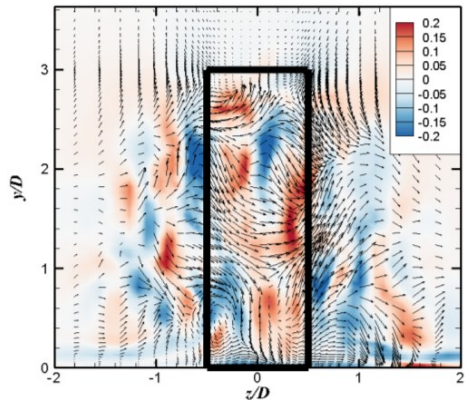

(a)

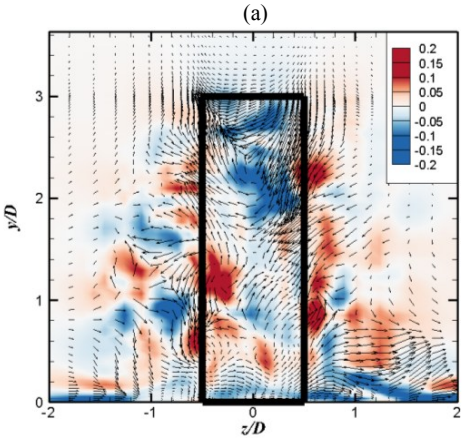

(b)

Figure 5. Vorticity ($\omega_x D/U_\infty$) contours superimposed over the velocity vectors (w,v) for the (a) 1st energy mode, and (b) 2nd energy mode in the transverse plane x/D = 3.5.

Figure 7 shows the plots of the reconstructed velocity field in the transverse plane at x/D = 3.5 for three different snapshots as viewed from upstream of the prism with the freestream velocity direction going into the plane of the figure. The snapshots are separated by approximately one-eighth of a period. Each velocity field was generated using an instantaneous POD reconstruction employing the first ten energy modes, and contours of streamwise vorticity were used to identify vortex structures. Since vorticity contours may sometimes be misleading in flows dominated by shearing effects, the swirling strength criterion was also employed, with the limitation that it cannot predict the orientation of the captured vortex structures. Figure 8 shows the corresponding swirling strength criterion plots for the same velocity fields considered in Figure 7. Overall, comparison of the two figures indicates that the strongest contours of streamwise vorticity identify the same vortex structures that are captured by the swirling strength criterion.

In Figure 7(a), we observe two distinct counter-rotating vortices next to each other just below the free-end of the prism. For this snapshot, their interaction results in a local upwash flow along the vertical centerline of the prism, which is opposite to the downwash flow present in the time-averaged velocity field. The location and sign of these vortices change in the next two snapshots. In the second snapshot, Figure 7(b), only a single vortex is present, while in the third snapshot, Figure 7(c), a vortex pair is present but with the sign of the vorticity reversed, so that we now observe a downwash flow consistent with the hypothesis of tip vortices seen in previous studies. Each axial vortex might be associated with the junction of a connector strand to the principal core of a half-loop. However, this would not explain why two vortices are sometimes observed in the same plane, or why the sign of the vorticity changes. It may be that the location of the transverse plane is too close to the prism for the half-loop structures to have developed at this downstream location.

The lower region of the wake for the snapshots shown in Figures 7 and 8 contains an assortment of smaller vortices. Typically their lateral distribution increases with proximity to the ground plane. Some of the vortices located in the central region of the wake may represent the intersection of the transverse plane with a connector strand, but without further analysis this cannot be confirmed.

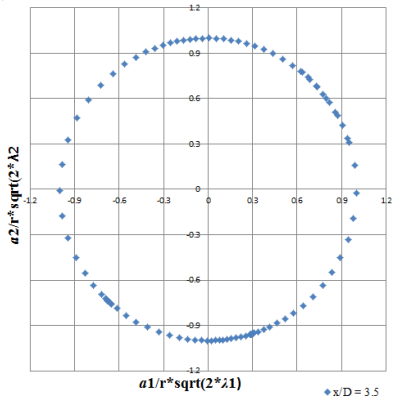

Figure 6. Correlation of first two normalized POD temporal coefficients (a_1^*, a_2^*) for x/D = 3.5 plane

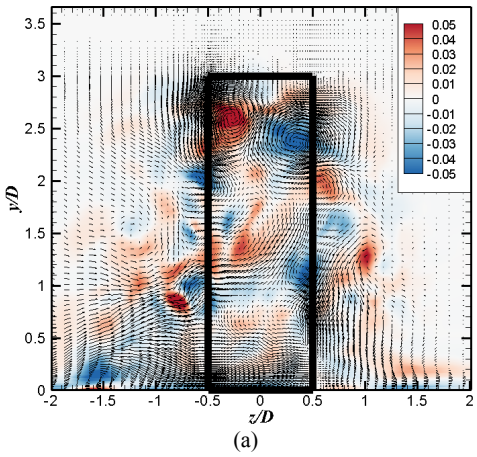

(a)

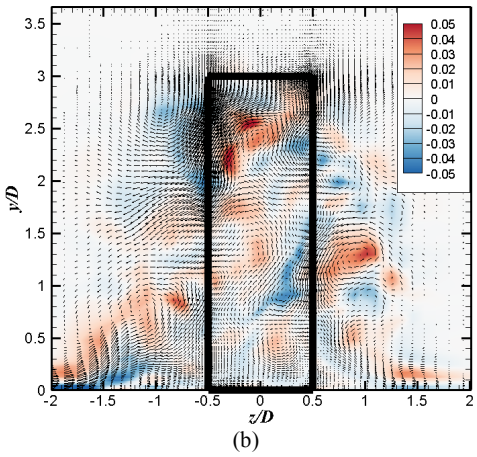

(b)

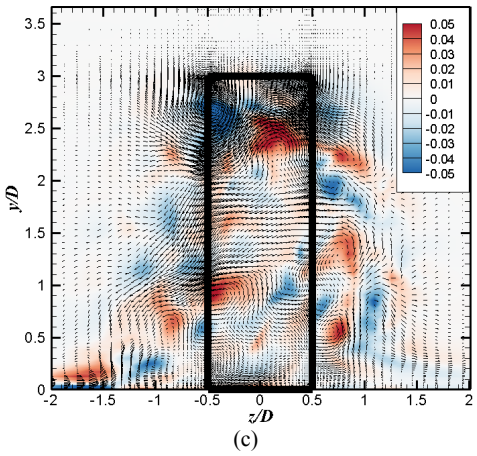

(c)

Figure 7. Vorticity ($\omega_x D/U_\infty$) contours superimposed over the velocity vectors (w,v) for the reconstructed flow field in the transverse plane x/D = 3.5 for three snapshots (a), (b) and (c) separated by an eighth of a time period.

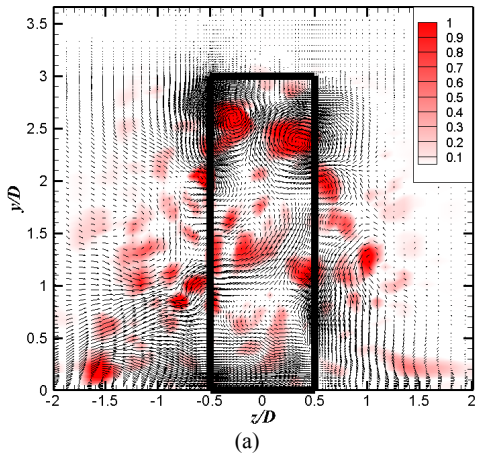

(a)

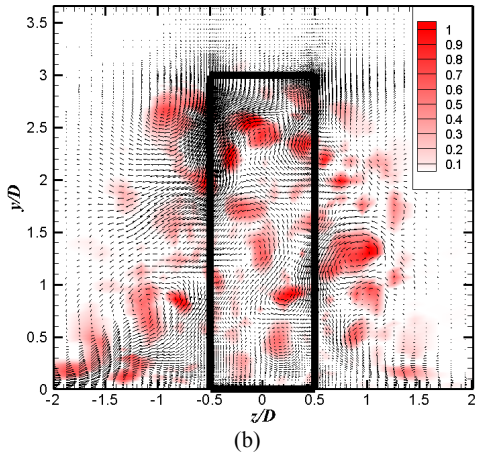

(b)

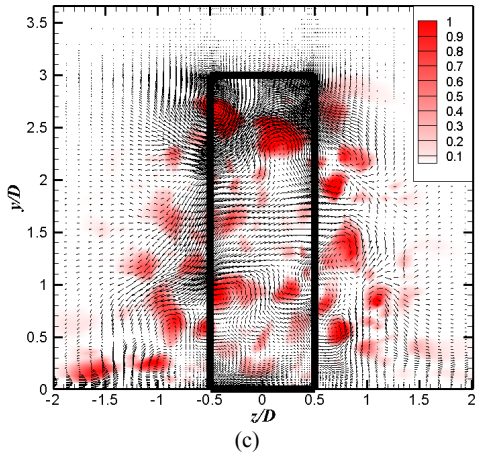

(c)

Figure 8. Swirling strength criterion contours superimposed over the velocity vectors (w,v) for the reconstructed flow field in the transverse plane x/D = 3.5 for three snapshots (a), (b) and (c) separated by an eighth of a time period.

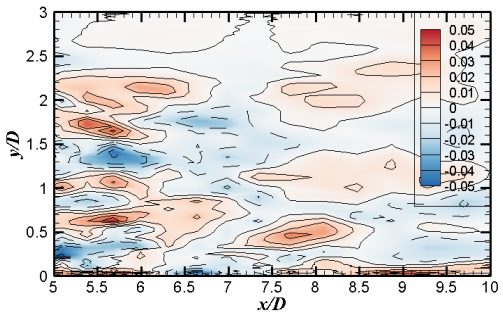

Figure 9. Vorticity ($\omega_z D/U_\infty$) contour lines and flood distribution for the wake (x/D > 5) reconstructed flow field in the transverse mid-plane z/D = 0 for a random instantaneous snapshot.

Figure 4 indicates that for the mid-plane located at z/D = 0, the first four modes have a similar energy content. This suggests that a POD reconstruction using the first four energy modes in this plane would yield some dominant flow structures. Figure 9 shows the transverse or z-vorticity contours in the mid-plane for a given snapshot based on POD reconstructions using the first four modes. The plot considers the region downstream of the near-wake, which is dominated by a large recirculation zone, see Figure 2. Figure 9 shows a distribution of vortices, most of which are stretched in the streamwise direction. Some of these might be indicative of a connector strand crossing the mid-plane of the wake. Recall that the connector strand joins two principal cores, located on opposite sides of the wake. As the half-loop moves downstream in the wake, the connector strand would be represented by a weak vortex structure in the mid-plane, which moves closer to the ground plane as the half-loop moves downstream. Again, further analysis and phase-averaging over multiple periods would be required to confirm whether the vortices observed in Figure 9 represent the signature of a connector strand.

CONCLUSIONS

POD analysis was used to study the wake created by a low Reynolds number flow over a finite-height square prism (AR = 3) mounted on a ground-plane. The instantaneous velocity field, obtained from an LES, was sampled to provide 100 POD snapshots equally spaced in time and spanning a little more than one shedding period. Vorticity and swirling strength criterion were used to identify the vortex structures in two sampling planes located in the wake of the prism. The sampling planes consisted of the vertical mid-plane of the wake, and a transverse section located 3.5D downstream of the prism. The intent was to use the POD to identify two-dimensional vortex patterns that might be associated with the half-loop structures which have been proposed as a structural model for these flows.

The energy distribution of the POD modes in each plane indicated that the flow was dominated by a small subset of modes. The POD coefficients indicated that the transverse plane was characterised by strong periodicity associated with the shedding frequency, whereas for the mid-plane a similar periodic behaviour was not observed.

The instantaneous velocity field in the transverse plane was reconstructed for different snapshots using just ten POD modes. The reconstructed velocity fields were dominated by strong vortex structures located near the top of the cylinder. These typically, but not always, occurred as a pair of counter-rotating vortices, and were reminiscent of the so-called tip vortices frequently identified in studies of the mean flow. However, the sign of the vorticity varied, so that flows with both upwash and downwash velocities along the centerline of the wake were observed.

A similar analysis in the mid-plane proved far more challenging, as this plane showed a more complex periodic pattern and revealed no definitive structures consistent with those previously documented in the literature. Neither of the planes considered gave compelling evidence of the presence of half-loop structures. However, it may well be that a more refined analysis and larger data sets will be required to identify these structures.

ACKNOWLEDGEMENTS

The support of the Natural Sciences and Engineering Research Council of Canada is gratefully acknowledged.

REFERENCES

[1] Wang, H. F., and Zhou, Y., 2009, "The finite-length square cylinder near wake", *Journal of Fluid Mechanics*, Vol. 638, pp. 453-490.

[2] Bourgeois, J. A., Sattari, P., and Martinuzzi, R. J., 2011, "Alternating half-loop shedding in the turbulent wake of a finite surface-mounted square cylinder with a thin boundary layer", *Physics of Fluids*, Vol. 23.9, pp. 095101.

[3] Saha, A. K., 2013, "Unsteady flow past a finite square cylinder mounted on a wall at low Reynolds number", *Computers & Fluids*, Vol. 88, pp. 599-615.

[4] Sirovich, L., 1987, "Method of snapshots", *Q. Appl. Math*, Vol. 45, pp. 561-571.

[5] Van Oudheusden, B. W., Scarano, F., Van Hinsberg, N. P., & Watt, D. W., 2005. "Phase-resolved characterization of vortex shedding in the near wake of a square-section cylinder at incidence", *Experiments in Fluids*, Vol. 39(1), pp. 86-98.

[6] Chong, M. S., Perry, A. E., and Cantwell, B. J., 1990, "A general classification of three-dimensional flow fields", *Physics of Fluids A: Fluid Dynamics*, Vol. 2.5, pp. 765-777.

[7] Wang, H. F., Cao, H. L., and Zhou, Y., 2014, "POD analysis of a finite-length cylinder near wake", *Experiments in Fluids*, Vol. 55.8, pp. 1-15.

[8] Okajima, A., 1982, "Strouhal numbers of rectangular cylinders", *Journal of Fluid Mechanics*, Vol. 123, pp. 379-398.